ORIGINAL ARTICLE - ELECTRONICS, MAGNETICS AND PHOTONICS

A Soluble 'Ba(Ni-ett)' (ett = 1,1,2,2-Ethenetetrathiolate) Derived Thermoelectric Material

Yaoyang Hu[1] · Geoffrey Rivers[2] · Michael P. Weir[3] · David B. Amabilino[4] · Christopher J. Tuck[2] · Ricky D. Wildman[2] · Oleg Makarovsky[3] · Simon Woodward[1]

Abstract

We describe the synthesis and characterisation of the first of a new class of soluble ladder oligomeric thermoelectric material based on previously unutilised ethene-1,1,2,2-tetrasulfonic acid. Reaction of $Ba(OH)_2$ and propionic acid at a 1:1 stoichiometry leads to the formation of the previously unrecognised soluble $[Ba(OH)(O_2CEt)]\cdot H_2O$. The latter when used to hydrolyse 1,3,4,6-tetrathiapentalene-2,5-dione (TPD), in the presence of $NiCl_2$, forms a new material whose elemental composition is in accord with the formula $[(EtCO_2Ba)_4Ni_8\{(O_3S)_2C=C(SO_3)_2\}_5]\cdot 22H_2O$ (**4**). Compound **4** can be pressed into pellets, drop-cast as DMSO solutions or ink-jet printed (down to sub-mm resolutions). While its room temperature thermoelectric properties are modest (σ_{max} 0.04 S cm^{-1} and Seebeck coefficient, α_{max} -25.8 µV K^{-1}) we introduce a versatile new oligomeric material that opens new possible synthetic routes for n-type thermoelectrics.

Graphical Abstract
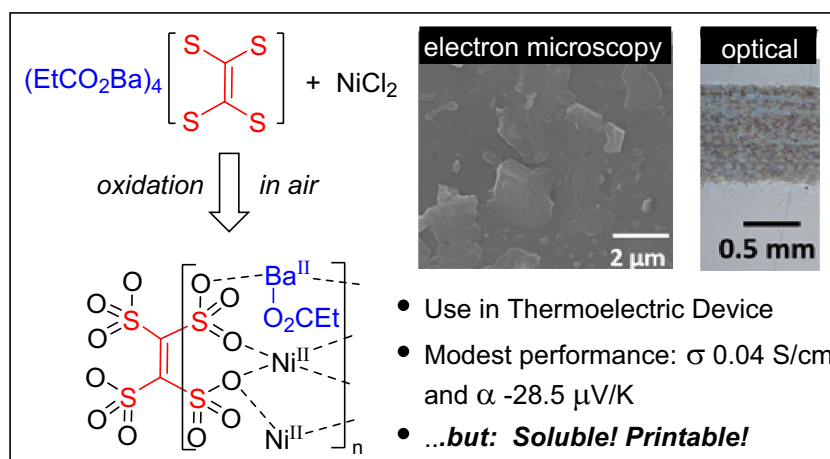
✉ Yaoyang Hu
yaoyang.hu@nottingham.ac.uk; yaoyanghuchem@gmail.com

✉ Michael P. Weir
michael.weir@nottingham.ac.uk

1   GSK Carbon Neutral Laboratories for Sustainable Chemistry, University of Nottingham, Jubilee Campus, Nottingham NG7 2TU, UK
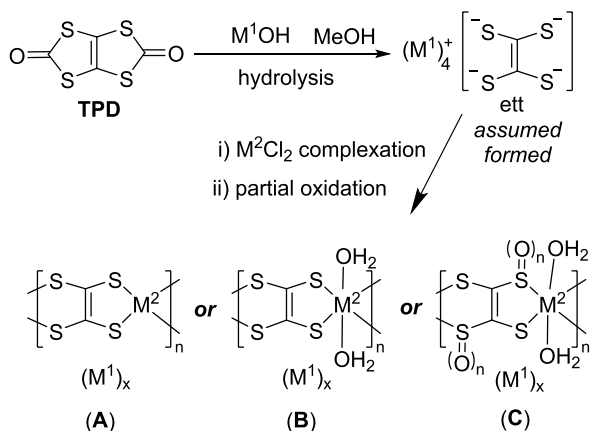
2   Faculty of Engineering, University of Nottingham, Nottingham NG7 2RD, UK

3   School of Physics and Astronomy, University of Nottingham, Nottingham NG7 2RD, UK

4   Institut de Ciència de Materials de Barcelona (ICMAB-CSIC), Consejo Superior de Investigaciones Científicas, Campus Universitari de Bellaterra, 08193 Cerdanyola del Vallès, Spain

1 Introduction

Zhu's [1] 2012 re-evaluation of earth-abundant poly-[$M^1_x(M^2$-ett)][2] complexes (ett = 1,1,2,2-ethenetetrathiolate; M^1 = Na, K; M^2 = Ni, Cu; typically with x = 0.02–0.25, but as high as 0.6, Scheme 1) as thermoelectric (TE) materials has generated wide interest. This is as a result of their high potential for use in sustainable heat-to-power energy harvesting devices [3–6]. In particular, the excellent TE performance of poly-[K_x(Ni-ett)] is attractive, because of its high air stability, which is rare in n-type carriers [7–15]. However, two significant limitations of such materials exist: their poor solubility and potential to form diverse (unpredictable) microstructures hindering their use. Poly-[$M^1_x(M^2$-ett)] materials precipitate very rapidly when their in situ reaction precursors are exposed to air (Scheme 1). This leads to a distribution of material compositions and particle sizes that is dependent on the reaction micro-conditions. Variation in TE performance for samples nominally prepared under identical conditions can result. The complete insolubility of poly-[$M^1_x(M^2$-ett)] complexes also prevents subsequent solution-based purification and re-processing and hinders chemical characterisation of the materials. Poly-[$M^1_x(M^2$-ett)] complexes are typically represented as 1D ladder polymers containing structural motif **A** (Scheme 1) in the literature, but this is a significant simplification. Recent XPS studies led to the realisation that both hydrated (**B**) and oxidised ett (**C**) polymer forms can also be present [16]. Based on their elemental analyses, additional (presently poorly characterised) impurities can also be present within poly-[$M^1_x(M^2$-ett)] samples. Finally, full characterisation of the materials is further complicated by the redox-active nature of the ett ligand itself (i.e. its ability to provide oxidised tetrathiooxalate units in situ) [17]. These factors make rational design of new metal-ett TE materials presently challenging.

Colloidal suspensions of poly-[K_x(Ni-ett)] can sometimes be used to prepare film devices which show a range of TE properties (Table 1) [18–24]. Aqueous ethylene glycol micro suspensions currently offer the best approach (Table 1, fourth entry) [21]. However, a truly homogeneous form of 'Ni(ett)' would be attractive, as this would allow improved characterisation, film casting and ink-jet printing approaches to device fabrication. Only extruded pastes or suspensions of Ni-ett materials are presently used to prepare simple TE modules (Table 1) [18–24]. As opportunities to modify the

Approximate [$M^1(M^2$-ett)] polymer composition	motif	σ_{rt} (S cm^{-1})	α_{rt} (μV K^{-1})	PF_{rt} (μW m^{-1}K^{-2})
~ Na$_6$(Ni$_{24}$-ett$_{24}$)•$_{23}$H$_2$O	A,B	40	-75	23
~ K(Ni$_{44}$-ett$_{49}$)•$_{50}$H$_2$O	A,B	44	-122	66
~ Na$_{11}$(Ni$_{47}$-ett$_{40}$)•$_{45}$H$_2$O	A,B	7	-84	5
~ Na$_6$(Cu$_6$-ett$_6$)•$_7$H$_2$O	A,B	0.2	79	0.1
~ Na$_2$(Cu$_{47}$-ett$_{24}$)O$_{39}$•$_7$H$_2$O	C	9.5	83	6.5

Scheme 1 Preparation and thermoelectric properties of Zhu's[1] original $M^1_x[M^2$(ett)] species: σ_{rt}, α_{rt}, and PF_{rt} are the room temperature electrical conductivity, Seebeck coefficient and Power Factor respectively. The empirical formulae presented are the best (linear least squares) fits attained to the bulk material C, H and metal elemental analysis data provided by Zhu[1] (ΔC%$_{error}$ 0.1–3.3%, ΔH%$_{error}$ 0.1–0.7, $\Delta M^1/M^2$%$_{error}$ 0.2–3.3. **TPD** = 1,3,4,6-tetrathiapentalene-2,5-dione

Table 1 Comparative thermoelectric performance of known 'Ni-ett' formulated films

Material	Dry/anneal temp (°C)	σ_{max} (S cm^{-1})	α_{max} (μV K^{-1})	PF_{max} (μW m^{-1} K^{-2})	References
[K_x(Ni-ett)]$_n$ ball milled with PVDF	90	2	− 36	0.26	[18]
[Na_x(N-ett)]$_n$ with ionic liquid BMIMBF	rt	~10–3	–	–	[19]
37 nm particles of [Na_x(N-ett)$_n$] with PVC	60	4.4×10^{-3}	−36	5.7×10^{-4}	[20]
190 nm [Na_x(N-ett)$_n$] + iodine in EG	210	52	−79	33	[21]
[Ni-tto]$_n$ ball milled with PVDF	160	90	−20	3.6	[22]
[K_x (Ni-ett)]$_n$ ball milled with PVDF	60	0.5	−28	4.1×10^{-2}	[23]
[Na_x(N-ett)]$_n$ particles with CNT and PVC	60	630	+30	58.6	[24]

PVDF polyvinylidene fluoride, *BMIM* butyl-methyl-1*H*-imidazol-3-ium, *PVC* polyvinyl chloride, *EG* ethylene glycol, *tto* tetrathiooxalate (oxidised ett), *CNT* carbon nanotubes

structure of the ett ligand itself (to improve solubility) are not available, we considered a new strategy to solubilise 'Ni-ett' species through use of barium carboxylate salts. Barium is the most sustainable of the heavy elements in the periodic table [25, 26] and, potentially offers additional opportunities for improving thermoelectric performance by a range of effects, such as carrier filtering, as has been observed in some related non-composite materials [27].

2 Experimental

Full experimental details of all materials prepared and their characterisation are described in the Supporting Information.

3 Results and Discussion

3.1 Synthesis and Characterisation

We began our studies by identifying an appropriate barium-based carboxylate with which to carry out the hydrolysis of TPD (Scheme 2, TPD = 1,3,4,6-tetrathiapentalene-2,5-dione), as this is commonly used to access ett. Preliminary studies revealed that pre-mixture of $Ba(OH)_2$ and equimolar amounts of $EtCO_2H$ provided the best hydrolysis conditions. Unexpectedly, such mixtures do not remain as separate distinct phases but react overnight to form previously unrecognised $[(EtCO_2)BaOH]\cdot H_2O$ (2). We make this assignment on the basis of the shift of the IR carbonyl (C = O) stretching frequency from 1708 cm^{-1} in propionic acid to 1535 cm^{-1} in $[(EtCO_2)BaOH]\cdot H_2O$ (2), which is expected upon barium coordination of the carboxylate [28]. Power X-ray diffraction confirms that $Ba(OH)_2$ is absent (against authentic samples) and that a new crystalline phase attributed to $[(EtCO_2)BaOH]\cdot H_2O$ (2) is present in the solid state. Finally, $[(EtCO_2)BaOH]\cdot H_2O$ (2) is completely soluble in methanol-d_4 (unlike barium hydroxide propionic acid mixtures) and its ^{13}C NMR carbonyl resonance (183.5 ppm) is significantly shifted from propionic acid (178.7 ppm) in the same solvent. The carboxylate peak for (2) is also reproducibly shifted + 0.2 ppm higher than that of authentic, independently prepared, $Ba(O_2CEt)_2$ recorded under identical conditions (see Supporting Information). All of these facts indicate (2) is a separate phase, not simple admixture of $Ba(OH)_2$ and $Ba(O_2CEt)_2$. We believe the reason (2) has remained unrecognised is that its elemental analysis and that of a simple 1:1 admixture of the starting materials give identical values. Attempts to remove the water of crystallisation from (2) at 80 °C for 16 h led to *ca.* 18% BaO formation based of the CHN analyses of such samples. Barium metal analyses of (2) are also consistent with the proposed formulation.
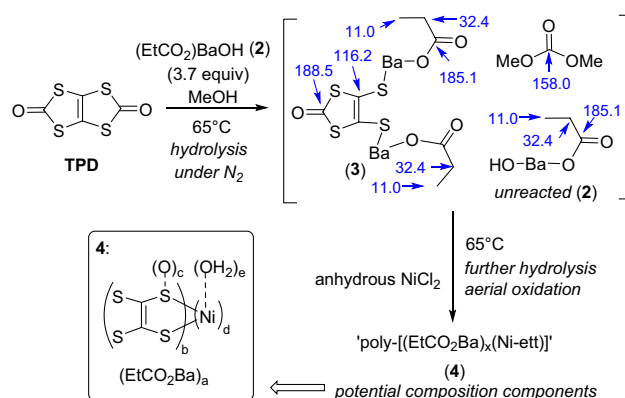
Scheme 2 Partial hydrolysis of TPD with $(EtCO_2)BaOH$ (2) in methanol at 65 °C and reaction of the intermediate (2/3) mixture to form compound 4 though further hydrolysis and aerial oxidation in the presence $NiCl_2$. The blue text, within the (2/3) structures show the ^{13}C NMR signals (ppm) observed after 16 h. **TPD** = 1,3,4,6-tetrathia-pentalene-2,5-dione

We used freshly prepared (2) to hydrolyse TPD (Scheme 2), in place of M^1OH (M = Na, K). A 3.7:1 ratio of (2): TPD was employed in order to be sure that all of the barium carboxylate was consumed, so that no unreacted excesses of barium carboxylates are present to complicate the analysis of the final nickel material. Overnight heating (16 h) at 65 °C led to complete consumption of the TPD, as monitored by ^{13}C NMR. Based on the work of Tkachov [13], we assign the remaining signals observed in the ^{13}C NMR spectrum (188.5, 185.1, 158.0, 116.2, 32.4, and 11.0 ppm) of the reaction mixture to the species given in Scheme 2. Subsequent addition of anhydrous $NiCl_2$ causes the reaction solution to become very dark. After additional heating (65 °C, 24 h) the TPD-intermediate 3 and unreacted 2 are completely consumed leading to fine black precipitate that was initially ascribed to 'poly-$[(EtCO_2Ba)_x(Ni-ett)]$' (4). This is easily isolated after addition of water and filtration in air (Scheme 2).

Material (4) was analysed by CHN combustion analysis, supported by barium and nickel metal analyses by inductively coupled plasma-optical emission spectrometry (ICP-OES). These data were used to attain best fits (linear regression) to the stoichiometry coefficients *a-e* shown in the box in Scheme 2. The data are in accord with a composition $[(EtCO_2Ba)_4(ett)_5O_{60}Ni_8]\cdot 22H_2O$ for (4). The presence of the initially unexpectedly high O:S ratio is confirmed by Energy Dispersive X-Ray Analysis (EDX) studies of pressed pellets of (4) (1000 bar, 5 min) (Supporting Information) which also support the proposed formulation. No chlorine signal is seen in the EDX spectrum of (4), indicating complete substitution of $NiCl_2$ (Fig. 1.). Consistent with this picture (4), digested in HNO_3, gives a negative chloride test with $AgNO_3$. Solid-state FTIR studies of (4), as isolated,
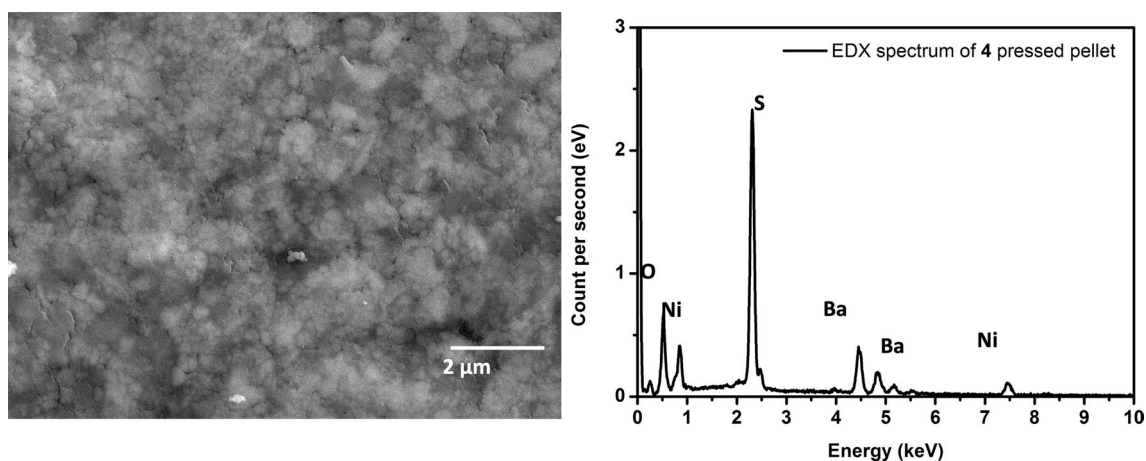
Fig. 1 A representative electron microscopy image of $[(EtCO_2Ba)_4Ni_8\{(O_3S)_2C=C(SO_3)_2\}_5]\cdot 22H_2O$ (**4**) pressed pellet and its associated EDX spectrum

reveal the presence of new strong bands at 1422 and 1078 cm^{-1}. Typically organosulfonyl RSO_3 units show strong asymmetric/symmetric $\nu_{S=O}$ stretches at 1200–1400 cm^{-1} and around 1050 cm^{-1} respectively [29–31]. Overall, these observations indicate that extensive aerial oxidation takes place during the isolation of **4** in air causing all of the ett thiols to become converted to $[(O_3S)_2C=C(SO_3)_2]^{4-}$. The latter ligand has been described once in the literature, during CO_2 reduction studies as its tetrasodium salt [32], but its IR spectrum is not described. Our elemental H, C, Ni, O, S and Ba analyses of (**4**) are in good agreement with formulation as $[(EtCO_2Ba)_4Ni_8\{(O_3S)_2C=C(SO_3)_2\}_5]\cdot 22H_2O$ (see Supporting Information). We attribute the aerobic thiol oxidation behaviour to the presence of our soluble barium intermediates, as completely insoluble poly-$[K_x(Ni-ett)]$ is only oxidised slowly in the solid state under vigorous conditions (200 °C) after its isolation [16]. In control reactions when we hydrolysed TPD with $Ba(OH)_2$ alone and this led only to poorly characterisable insoluble materials, completely unrelated to (**4**).

In agreement with its polar formulation, unlike the species **A–C** (Scheme 1), (**4**) is fully soluble in DMSO and partially in other polar solvents. UV–vis–NIR spectra of (**4**) (DMSO 10^{-4} M) show peaks at $\lambda_{max}=313$ and 375 nm, close to reported literature value for π–π^* transition of ett-type ligands, respectively [33, 34]. Two broad peaks 1070 and 1263 nm, the latter trailing off into long wavelength infra-red, beyond the detector range of our instrument (1400 nm) are suggestive of charge transfer events [19]. Using the frequency of the latter peak as an approximate band gap transition energy gives an E_g(opt) estimate for (**4**) of ≤ 1 eV. This is similar to the values that have been calculated for a range of related nickel conducting oligomers (both known and hypothetical) [35]. The magnetic susceptibility (χ_g) of material (**4**), as isolated, gives $\chi_g = 3.17 \times 10^{-8}$ m^3

kg^{-1} by standard Evan's balance measurements, indicating (**4**) is paramagnetic. This prevents detection of ett-derived ligands by ^{13}C NMR spectroscopy, but the propionate ethyl groups could be seen in the proton NMR studies, although they were significantly broadened. Quantification against a 1,2-dibromoethane internal standard indicated 4–5 wt% of (**4**) to be 'EtCO_2', compared to the 8.5 wt% calculated for the formula: $[(EtCO_2Ba)_4Ni_8\{(O_3S)_2C=C(SO_3)_2\}_5]\cdot 22H_2O$ (**4**). However, it was not possible to measure t_1 relaxation values for (**4**) and relaxation differences between the 1,2-dibromoethane standards and paramagnetic (**4**), are likely to be significant and affect the relative integrals significantly.

As we were unable to grow crystals of (**4**), we sought to visualise (at least potential) structures for it via space-filling molecular models (see Supporting Information). The linear 'pentamers' (**4a/b**) realised from this are in accord with the elemental analysis and other (composition) data (Scheme 3) observed. We prefer the former of these (**4a**) as a simple working model, due to the lack of steric clashes. However, both forms did indicate the viability of discrete, soluble, coordination clusters consistent with the analytical data attained (in the absence of crystallographic data). The true nature of (**4**) is undoubtedly more complex than this simple model and other oligomer lengths and degrees of coordination/oxidation are possible. Our isolated samples of (**4**) are thus likely a mixture of species, but with cores all related to (**4a/b**).

3.2 Formulation of (4) and thermoelectric properties

The powder form of (**4**) could be easily pressed into a pellet (diameter 4 mm × 139 μm deep), and its electrical conductivity and Seebeck coefficient determined by standard means (Table 2; further information on the techniques

(4a) **(4b)**
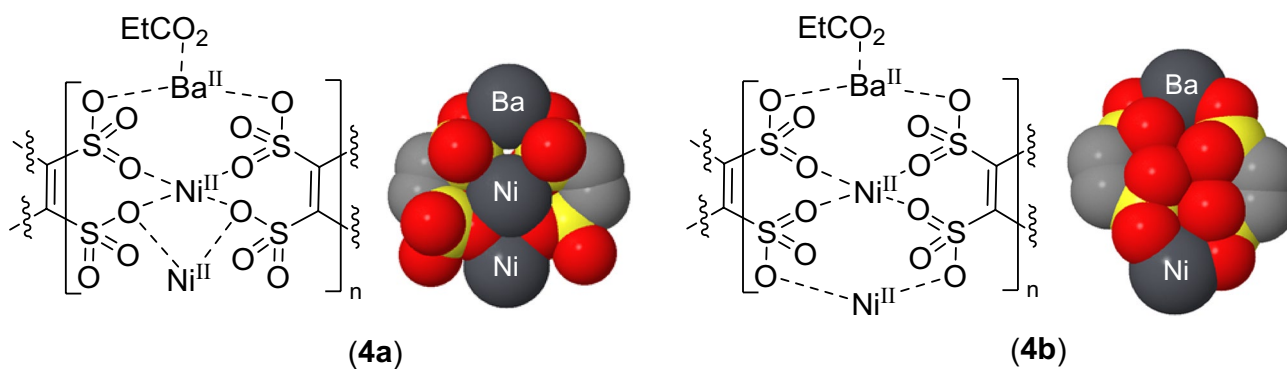
Scheme 3 Core of the proposed structure ladder motif in compound **4**, free coordination sites are assumed to be water or solvent occupied. Structures with a bridging μ-O sulfate (**4a**) lead to a planar [(EtCO$_2$B a)$_4$Ni$_8${(O$_3$S)$_2$C=C(SO$_3$)$_2$}$_5$] units, while motif (**4b**) was disfavoured, leading to overly close sulfonyl oxygen contacts and deviations from planarity

Table 2 Thermoelectric properties of pressed pellet vs. drop-cast and ink-jet printed films of [(EtCO$_2$Ba)$_4$Ni$_8${(O$_3$S)$_2$C=C(SO$_3$)$_2$}$_5$]·22H$_2$O (**4**)[a]

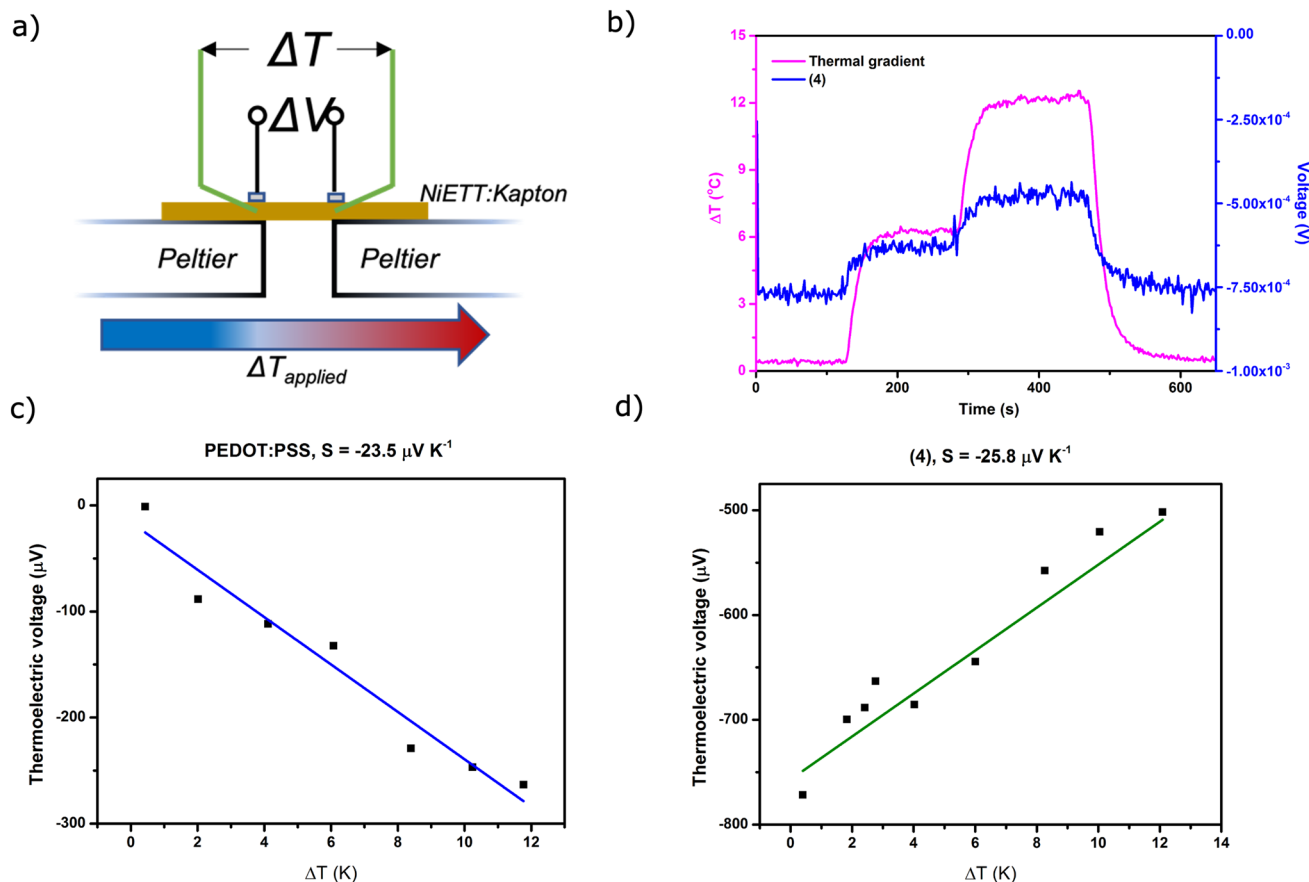| Formulation of (4)	Dry/anneal temp (°C)	σ_{max} (S cm^{-1})	α_{max} (μV K^{-1})	PF$_{max}$ (μW m^{-1} K^{-2})
Pressed pellet (1000 bar, 5A min)	80	3.7×10^{-2}	-24.3	21.8×10^{-3}
DMSO drop-cast 11 μm film	150	4.0×10^{-2}	-25.9	26.8×10^{-3}
BuOH/DMSO printed 0.7 μm film	150	1.14×10^{-2}	-25.8	7.6×10^{-3}

Fig. 2 Lateral Seebeck measurements of printed lines of PEDOT:PSS and **4**, showing **a** schematic of the experimental setup, **b** thermoelectric voltage vs. time for **4** and graphs of thermoelectric voltage vs ΔT for **c** the PEDOT:PSS printed line and **d** the **4** printed line, both including a linear fits to the data, the gradient of which is equal to -S

Fig. 3 Three-junction [(EtCO$_2$Ba)$_4$Ni$_8${(O$_3$S)$_2$C═C(SO$_3$)$_2$}$_5$]·22H$_2$O (**4**)/PEDOT-PSS TE device, showing the architecture and optical microscope images of the printed lines
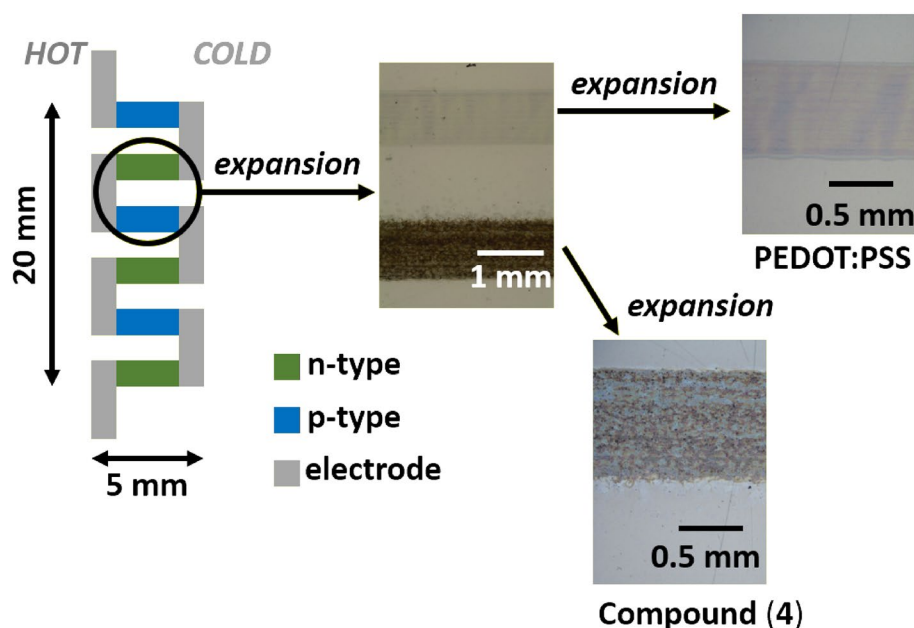
employed are provided in the Supporting Information). A summary of the approach used to measure the thermoelectric properties is presented in Fig. 2. DMSO solutions of (**4**, 0.22 M) could also be easily drop cast onto Kapton tape, resulting in films around 10 µm thick. The thermoelectric properties of both the pellets and films were investigated (Table 2). Finally, the surface tension and viscosity of DMSO solutions of (**4**) are, when co-mixed with *n*-butanol (BuOH), appropriate for ink-jet printing of thin films, whose headline properties are reported in Table 2 (other mixtures were also investigated, see Supporting Information). Annealing of these thin films was required in all cases to attain n-type TE materials.

Clearly, while the performance of (**4**) is inferior to the current best 'Ni-ett' nanoparticle/PVDF formulations in power factor (PF$_{max}$ = 58.6 µW m^{-1}K^{-2}, [24] see Table 1), it does afford opportunities for simplifications in multi-junction device preparation. To investigate this, we prepared a 3-junction device using (**4**) for the n-type and commercial PEDOT-PSS for the p-type material. Printing resolutions of ca. 1 mm are easily attained (Fig. 3) on to PEN (polyethylene naphthalate) as a flexible substrate. For details of the optimisation of the printing conditions and associated Hansen/Jettability plots see the Supporting Information. At a temperature difference of 7.9 °C this simple device delivered an output of -93.1 µV K^{-1}. Microscopy of the printed films revealed some aggregation of material (**4**) occurs during its drying (see Supporting Information). The resultant minor film defects do have a minor negative (grain boundary) effect on the devices, but in no case do the films fall below their electrical percolation limits.

4 Conclusion

Our simple idea that the potassium counter cation in poly-[K$_x$(Ni-ett)] could be replaced by a barium carboxylate, solubilising the material, has been fulfilled. Compound **4** is, to the best of our knowledge, the first organic coordination oligomer containing barium to have its TE properties extensively investigated [36, 37]. Including EtCO$_2$Ba units provides a 'poly-[(EtCO$_2$Ba)$_x$(Ni-ett)]' material that is soluble in polar solvents (primarily DMSO). Elemental analysis reveals the reason for this to be induced aerobic oxidation of the ett thiols to sulfonic acids and that the isolated material is, in fact, an oligomer of the composition [(EtCO$_2$Ba)$_4$Ni$_8${(O$_3$S)$_2$C═C(SO$_3$)$_2$}$_5$]·22H$_2$O (**4**). Although only partially related to known Ni-ett species this compound retains n-type behaviour and contains the fortuitously discovered ligand [(O$_3$S)$_2$C═C(SO$_3$)$_2$]$^{4-}$,[32] whose coordination polymers have not been described before. We propose that the latter has significant potential for use in dimensionally restricted (ladder) TE materials and other electrical conductors, and these we are currently investigating.

Declarations

Conflict of Interests The authors have no competing interests to declare.

References

1. Sun, Y., Sheng, P., Di, C., Jiao, F., Xu, W., Qiu, D., Zhu, D.: Organic thermoelectric materials and devices based on p- and n-type poly(metal 1,1,2,2-ethenetetrathiolate)s. Adv. Mater. **24**, 932–937 (2012). https://doi.org/10.1002/adma.201104305

2. Poleschner, H., John, W., Hoppe, F., Fanghänel, E., Roth, S.: Tetrathiafulvalene. XIX. Synthese und Eigenschaften elektronenleitender Poly-Dithiolenkomplexe mit Ethylentetrathiolat und Tetrathiafulvalentetrathiolat als Brückenliganden. J. Für Prakt. Chemie. **325**, 957–975 (1983). https://doi.org/10.1002/prac.19833250612

3. Sun, Y., Xu, W., Di, C., Zhu, D.: Metal-organic complexes-towards promising organic thermoelectric materials. Synth. Met. **225**, 22–30 (2017). https://doi.org/10.1016/j.synthmet.2016.12.001

4. E. Redel, H. Baumgart, Thermoelectric porous MOF based hybrid materials, APL Mater. 8 (2020) 060902. https://doi.org/10.1063/5.0004699.

5. Lu, Y., Young, D.J.: Coordination polymers for n-type thermoelectric applications. Dalt. Trans. **49**, 7644–7657 (2020). https://doi.org/10.1039/D0DT00872A

6. Massetti, M., Jiao, F., Ferguson, A.J., Zhao, D., Wijeratne, K., Würger, A., Blackburn, J.L., Crispin, X., Fabiano, S.: Unconventional thermoelectric materials for energy harvesting and sensing applications. Chem. Rev. **121**, 12465–12547 (2021). https://doi.org/10.1021/acs.chemrev.1c00218

7. Wan, K., Liu, Z., Schroeder, B.C., Chen, G., Santagiuliana, G., Papageorgiou, D.G., Zhang, H., Bilotti, E.: Highly stretchable and sensitive self-powered sensors based on the N-type thermoelectric effect of polyurethane/Nax(Ni-ett)n/graphene oxide composites. Compos. Commun. **28**, 100952 (2021). https://doi.org/10.1016/j.coco.2021.100952

8. Liu, Z., Liu, T., Savory, C.N., Jurado, J.P., Reparaz, J.S., Li, J., Pan, L., Faul, C.F.J., Parkin, I.P., Sankar, G., Matsuishi, S., Campoy-Quiles, M., Scanlon, D.O., Zwijnenburg, M.A., Fenwick, O., Schroeder, B.C.: Controlling the thermoelectric properties of organometallic coordination polymers via ligand design. Adv. Funct. Mater. **30**, 2003106 (2020). https://doi.org/10.1002/adfm.202003106

9. Wolfe, R.M.W., Menon, A.K., Marder, S.R., Reynolds, J.R., Yee, S.K.: Thermoelectric performance of n-type poly(Ni-tetrathiooxalate) as a counterpart to poly(Ni-ethenetetrathiolate): NiTTO versus NiETT. Adv. Electron. Mater. Lett. **5**, 1900066 (2019). https://doi.org/10.1002/aelm.201900066

10. Wolfe, R.M.W., Menon, A.K., Fletcher, T.R., Marder, S.R., Reynolds, J.R., Yee, S.K.: Simultaneous enhancement in electrical conductivity and thermopower of n-type NiETT/PVDF composite films by annealing. Adv. Funct. Mater. **28**, 1803275 (2018). https://doi.org/10.1002/adfm.201803275

11. Menon, A.K., Uzunlar, E., Wolfe, R.M.W., Reynolds, J.R., Marder, S.R., Yee, S.K.: Metallo-organic n-type thermoelectrics: Emphasizing advances in nickel-ethenetetrathiolates. J. Appl. Polym. Sci. (2017). https://doi.org/10.1002/app.44402

12. Tkachov, R., Stepien, L., Roch, A., Komber, H., Hennersdorf, F., Weigand, J.J., Bauer, I., Kiriy, A., Leyens, C.: Facile synthesis of potassium tetrathiooxalate – The "true" monomer for the preparation of electron-conductive poly(nickel-ethylenetetrathiolate). Tetrahedron **73**, 2250–2254 (2017). https://doi.org/10.1016/j.tet.2017.03.010

13. Tkachov, R., Stepien, L., Grafe, R., Guskova, O., Kiriy, A., Simon, F., Reith, H., Nielsch, K., Schierning, G., Kasinathan, D., Leyens, C.: Polyethenetetrathiolate or polytetrathiooxalate? Improved synthesis, a comparative analysis of a prominent thermoelectric polymer and implications to the charge transport mechanism. Polym. Chem. **9**, 4543–4555 (2018). https://doi.org/10.1039/C8PY00931G

14. Sun, Y., Qiu, L., Tang, L., Geng, H., Wang, H., Zhang, F., Huang, D., Xu, W., Yue, P., Guan, Y., Jiao, F., Sun, Y., Tang, D., Di, C., Yi, Y., Zhu, D.: Flexible n-type high-performance thermoelectric thin films of poly(nickel-ethylenetetrathiolate) prepared by an electrochemical method. Adv. Mater. **28**, 3351–3358 (2016). https://doi.org/10.1002/adma.201505922

15. Sun, Y., Zhang, J., Liu, L., Qin, Y., Sun, Y., Xu, W., Zhu, D.: Optimization of the thermoelectric properties of poly(nickel-ethylenetetrathiolate) synthesized via potentiostatic deposition. Sci. China Chem. **59**, 1323–1329 (2016). https://doi.org/10.1007/s11426-016-0175-9

16. Hwang, S., Potscavage, W.J., Jr., Kim, T.-W., Adachi, C.: Interplay among thermoelectric properties, atmospheric stability, and electronic structures in solution-deposited thin films of P(NaX[Niett]). Adv. Electron. Mater. Lett. **6**, 1901172 (2020). https://doi.org/10.1002/aelm.201901172

17. Wu, Y., Chen, Y., Tang, M., Zhu, S., Jiang, C., Zhuo, S., Wang, C.: A highly conductive conjugated coordination polymer for fast-charge sodium-ion batteries: reconsidering its structures. Chem. Commun. **55**, 10856–10859 (2019). https://doi.org/10.1039/C9CC05679C

18. Jiao F., Di C., Sun Y., Sheng P., Xu W., Zhu D.: Inkjet-printed flexible organic thin-film thermoelectric devices based on p- and n-type poly(metal 1,1,2,2-ethenetetrathiolate)s/polymer composites through ball-milling. Philos. Trans. R. Soc. A Math. Phys. Eng. Sci. 372, p. 20130008 (2014). https://doi.org/10.1098/rsta.2013.0008

19. Faulmann, C., Chahine, J., Jacob, K., Coppel, Y., Valade, L., de Caro, D.: Nickel ethylene tetrathiolate polymers as nanoparticles: a new synthesis for future applications? J. Nanoparticle Res. **15**, 1–18 (2013). https://doi.org/10.1007/s11051-013-1586-5

20. Oshima, K., Shiraishi, Y., Toshima, N.: Novel nanodispersed polymer complex, poly(nickel 1,1,2,2-ethenetetrathiolate): preparation and hybridization for n-type of organic thermoelectric materials. Chem. Lett. **44**, 1185–1187 (2015). https://doi.org/10.1246/cl.150328

21. Ueda, K., Yamada, Y., Terao, T., Manabe, K., Hirai, T., Asaumi, Y., Fujii, S., Kawano, S., Muraoka, M., Murata, M.: High-performance, air-stable, n-type thermoelectric films from a water-dispersed nickel-ethenetetrathiolate complex and ethylene glycol. J. Mater. Chem. A. **8**, 12319–12322 (2020). https://doi.org/10.1039/D0TA04524A

22. Tkachov, R., Stepien, L., Greifzu, M., Kiriy, A., Kiriy, N., Schüler, T., Schmiel, T., López, E., Brückner, F., Leyens, C.: A printable

paste based on a stable n-type poly[Ni-tto] semiconducting polymer. Coatings **9**, 764 (2019). https://doi.org/10.3390/coatings9110764

23. Menon, A.K., Meek, O., Eng, A.J., Yee, S.K.: Radial thermoelectric generator fabricated from n- and p-type conducting polymers. J. Appl. Polym. Sci. (2017). https://doi.org/10.1002/app.44060

24. Toshima, N., Oshima, K., Anno, H., Nishinaka, T., Ichikawa, S., Iwata, A., Shiraishi, Y.: Novel hybrid organic thermoelectric materials: three-component hybrid films consisting of a nanoparticle polymer complex, carbon nanotubes, and vinyl polymer. Adv. Mater. **27**, 2246–2251 (2015). https://doi.org/10.1002/adma.201405463

25. Anderson, D.L.: Chemical composition of the mantle. J. Geophys. Res. Solid Earth. **88**, B41–B52 (1983). https://doi.org/10.1029/JB088iS01p00B41

26. Hunt, A.J., Matharu, A.S., King, A.H., Clark, J.H.: The importance of elemental sustainability and critical element recovery. Green Chem. **17**, 1949–1950 (2015). https://doi.org/10.1039/C5GC90019K

27. Carvillo, P., Chen, Y., Boyle, C., Barnes, P.N., Song, X.: Thermoelectric performance enhancement of calcium cobaltite through barium grain boundary segregation. Inorg. Chem. **54**, 9027–9032 (2015). https://doi.org/10.1021/acs.inorgchem.5b01296

28. Drzewiecka-Antonik, A., Koziol, A.E., Rejmak, P., Lawniczak-Jablonska, K., Nittler, L., Lis, T.: Novel Ba(II) and Pb(II) coordination polymers based on citric acid: synthesis, crystal structure and DFT studies. Polyhedron **132**, 1–11 (2017). https://doi.org/10.1016/j.poly.2017.04.024

29. Levy, L.Y., Jenard, A., Hurwitz, H.D.: Infrared investigation of ionic hydration in ion-exchange membranes. Part 1.—Alkaline salts of grafted polystyrene sulphonic acid membranes. J. Chem. Soc. Faraday Trans. 1 Phys. Chem. Condens. Phases. 76: 2558–2574 (1980). https://doi.org/10.1039/F19807602558.

30. Peña, L., Xu, F., Hohn, K.L., Li, J., Wang, D.: Propyl-sulfonic acid functionalized nanoparticles as catalyst for pretreatment of corn stover. J. Biomater. Nanobiotechnol. **05**, 8–16 (2014). https://doi.org/10.4236/jbnb.2014.51002

31. Buzzoni, R., Bordiga, S., Ricchiardi, G., Spoto, G., Zecchina, A.: Interaction of H2O, CH3OH, (CH3)2O, CH3CN, and pyridine with the superacid perfluorosulfonic membrane nafion: an IR and Raman study. J. Phys. Chem. **99**, 11937–11951 (1995). https://doi.org/10.1021/j100031a023

32. Akiyama, F.: Evidence of conversion from carbon dioxide to unstable carbon oxides. Bull. Chem. Soc. Jpn. **63**, 2131–2133 (1990). https://doi.org/10.1246/bcsj.63.2131

33. Paes, L.W.C., Suárez, J.A., Márquez, A.M., Sanz, J.F.: First-principles study of nickel complex with 1,3-dithiole-2-thione-4,5-dithiolate ligands as model photosensitizers. Theor. Chem. Acc. **136**, 1–9 (2017). https://doi.org/10.1007/s00214-017-2098-7

34. da Cruz, A.G.B., Wardell, J.L., Simão, R.A., Rocco, A.M.: Preparation, structure and electrochemistry of a polypyrrole hybrid film with [Pd(dmit)2]2−, bis(1,3-dithiole-2-thione-4,5-dithiolate) palladate(II). Electrochim. Acta. **52**, 1899–1909 (2007). https://doi.org/10.1016/j.electacta.2006.07.061

35. Shi, W., Wu, G., Yong, X., Deng, T., Wang, J.-S., Zheng, J.-C., Xu, J., Sullivan, M.B., Yang, S.-W.: Orbital-engineering-based screening of π-conjugated d8 transition-metal coordination polymers for high-performance n-type thermoelectric applications. ACS Appl. Mater. Interfaces. **10**, 35306–35315 (2018). https://doi.org/10.1021/acsami.8b13877

36. Madhusudan, V., Sathyanarayan, S.G., Sastry, G.S.: Electrical conductivity and stimulated thermocurrent studies in dicalcium barium propionate single crystals. Phys. Status Solidi. **66**, 371–376 (1981). https://doi.org/10.1002/pssa.2210660145

37. Wing, H.J., Thompson, T.J.: The solubility of barium propionate. J. Am. Chem. Soc. **48**, 104–106 (1926). https://doi.org/10.1021/ja01412a014